

LA-UR- 08-4261

Approved for public release;
distribution is unlimited.

Title: First-principles study of $\text{Co}_3(\text{Al,W})$ alloys using special quasirandom structures

Author(s): Chao Jiang

Intended for: Scripta Materialia



Los Alamos National Laboratory, an affirmative action/equal opportunity employer, is operated by the Los Alamos National Security, LLC for the National Nuclear Security Administration of the U.S. Department of Energy under contract DE-AC52-06NA25396. By acceptance of this article, the publisher recognizes that the U.S. Government retains a nonexclusive, royalty-free license to publish or reproduce the published form of this contribution, or to allow others to do so, for U.S. Government purposes. Los Alamos National Laboratory requests that the publisher identify this article as work performed under the auspices of the U.S. Department of Energy. Los Alamos National Laboratory strongly supports academic freedom and a researcher's right to publish; as an institution, however, the Laboratory does not endorse the viewpoint of a publication or guarantee its technical correctness.

First-principles study of $\text{Co}_3(\text{Al},\text{W})$ alloys using special quasirandom structures

Chao Jiang*

Structure/Property Relations Group (MST-8), Los Alamos National Laboratory, Los Alamos, NM 87545

ABSTRACT

We develop 32-atom special quasirandom structures (SQS's) to model the substitutionally random pseudobinary $\text{A}_3(\text{B}_{0.5}\text{C}_{0.5})$ alloys in L1_2 , D0_{19} , and D0_3 crystal structures. The SQS's are employed to examine the phase stability of the recently identified $\text{L1}_2\text{-Co}_3\text{Al}_{0.5}\text{W}_{0.5}$ compound. Our first-principles calculations reveal that $\text{L1}_2\text{-Co}_3\text{Al}_{0.5}\text{W}_{0.5}$ is only marginally more stable than the $\text{D0}_{19}\text{-Co}_3\text{Al}_{0.5}\text{W}_{0.5}$ structure. Furthermore, it is not a thermodynamically stable phase at $T=0\text{K}$. Our predicted single-crystal elastic constants of $\text{L1}_2\text{-Co}_3\text{Al}_{0.5}\text{W}_{0.5}$ also show excellent agreement with recent experiments.

*Corresponding author: chao@lanl.gov

Co-base superalloys have long been believed to be impossible since there exists no stable $L1_2$ phase in the equilibrium Al-Co phase diagram [1]. Such a view has been challenged by the recent identification of a $Co_3(Al,W)$ compound with $L1_2$ crystal structure in the Co-Al-W ternary system, where the composition of Al and W has an almost equiatomic ratio [2]. Similar to $L1_2-Ni_3Al$ compound, $L1_2-Co_3Al_{0.5}W_{0.5}$ forms coherent cuboidal precipitates within the face-centered cubic (fcc) solid solution based on Co, thus enabling Co-base alloys to possess high temperature strength comparable to that of the commercial Ni-base superalloys [2, 3]. This discovery opens up the possibilities of future development of Co-base superalloys for high-temperature structural applications.

Since no thermodynamically stable phase with a $L1_2$ structure has been reported in any of the Co-Al, Co-W, and Al-W binary subsystems [1], it is desirable to use the highly predictive first-principles calculations based on density functional theory (DFT) to gain valuable insight into the phase stability of this newly discovered $L1_2-Co_3Al_{0.5}W_{0.5}$ compound. In our study, the full set of single-crystal elastic constants of $L1_2-Co_3Al_{0.5}W_{0.5}$ will also be predicted since such data are important for understanding its mechanical properties. Calculations are performed using the all-electron projector augmented wave method [4] within the generalized gradient approximation (PBE-GGA) [5], as implemented in VASP [6]. The semi-core $5p$ electrons of W are explicitly treated as valence. The electronic wavefunctions are expanded using a plane-wave basis set with a cutoff energy of 350 eV. The k -point meshes for Brillouin zone sampling are constructed using the Monkhorst–Pack scheme and the total number of k -points times the total number of atoms per unit cell is at least 10,000. All structures are fully relaxed using a conjugate-

gradient scheme. Our calculations are spin-polarized to account for the ferromagnetic nature of Co.

While it is straightforward to apply the DFT method to predict material properties of perfectly ordered structures [7], the situation is more complicated when treating disordered alloys such as $\text{Co}_3(\text{Al,W})$. The brute-force way to treat random A_{1-x}B_x solid solutions would be to construct a large supercell and randomly decorate the host lattice with A and B atoms. Nevertheless, such an approach requires very large supercells to adequately reproduce the statistics of random alloys and is computationally prohibitive for DFT calculations. To overcome such difficulties, we adopt the special quasirandom structure (SQS) approach proposed by Zunger *et al.* [8, 9]. SQS's are specially designed *small-unit-cell* periodic structures that closely mimic the most relevant near-neighbor pair and multisite correlation functions of random alloys. The advantage of the SQS approach over mean-field approaches such as the coherent potential approximation (CPA) [10] is that local environmentally-dependent effects such as charge transfer and local atomic relaxations can be accurately captured. Indeed, experiments [11] have shown that the average A–A, A–B and B–B bond lengths are generally different even in random A_{1-x}B_x solid solutions. Furthermore, local atomic relaxations have been shown to significantly affect the thermodynamic and electronic properties of size-mismatched semiconductor alloys [8, 9].

For a binary A_{1-x}B_x alloy, many physical properties such as energy are dependent on the *configuration*, or the substitutional arrangement of A and B atoms on the parent lattice.

The configuration dependence of properties can be efficiently characterized by a “lattice algebra”: Spin variables are assigned to each site, $S_i = -1 (+1)$ if A (B) sits at site i . A figure $f=(k, m)$ is defined as symmetry-related groupings of k lattice sites that span a maximum distance of m ($m=1, 2, \dots$ are the first and second-nearest neighbors, etc.). By taking the product of S_i over all sites of a figure, and averaging over all symmetry-equivalent figures of the lattice, the correlation functions $\bar{\Pi}_{k,m}$ is obtained [8, 9]. For a perfectly random $A_{1-x}B_x$ alloy, $\langle \bar{\Pi}_{k,m} \rangle_R = (2x-1)^k$ since there is no correlation in the occupation between various sites. The SQS approach is essentially finding small ordered structures that possess $\left(\bar{\Pi}_{k,m} \right)_{SQS} \cong \left(\bar{\Pi}_{k,m} \right)_R$ for as many figures as possible. Admittedly, describing random alloys by periodic SQS structures will surely introduce erroneous correlations beyond a certain distance. However, since interactions between widely separated atoms are expected to be weaker than interactions between nearer ones, we can construct SQS’s that exactly reproduce the near-neighbor correlation functions of a random alloy, deferring periodicity errors to more distant neighbors. As the size of the SQS’s becomes larger, such periodicity error diminishes and the SQS’s become increasingly better approximations of the real random alloy. In our previous studies [12, 13], we have observed rapid convergence of SQS calculated alloy properties with respect to SQS size, which strongly indicates that those properties are indeed dominated by the interactions between near neighbors. In such a case, even small SQS’s are already sufficient to provide reliable results.

Using ATAT [14], we have generated two SQS’s for random $L_{1/2} A_3(B_{0.5}C_{0.5})$ alloy: an orthorhombic-type SQS-1 structure (space group $Cmmm$) and a cubic-type SQS-2

structure (space group $Pm\bar{3}m$), whose pair correlation functions are identical to those of the random alloy up to the third and second-nearest neighbor, respectively (see Table 1). For $D0_{19} A_3(B_{0.5}C_{0.5})$, we have generated two orthorhombic-type SQS's: SQS-1 with space group $Amm2$ and SQS-2 with space group $Pmm2$, whose pair correlation functions match those of the random alloy up to the fourth and second-nearest neighbor, respectively. Finally, we have generated a monoclinic-type SQS with space group Pm for $D0_3 A_3(B_{0.5}C_{0.5})$, which accurately reproduces the pair correlation functions of the random alloy up to second-nearest neighbor. The pictures of our $L1_2$ SQS's are shown in Fig. 1 in their ideal, unrelaxed forms.

The development of the SQS's allows us to directly examine the phase stability of the $L1_2$ - $Co_3Al_{0.5}W_{0.5}$ compound. Fig. 2 shows our first-principles calculated formation energies of $Co_3Al_{1-x}W_x$ ($x=0, 0.5, 1$) alloys in various competing crystal structures. Here the formation energy of a $Co_{1-x-y}Al_xW_y$ alloy is defined as:

$$\Delta H = E(Co_{1-x-y}Al_xW_y) - (1-x-y)E(Co) - xE(Al) - yE(W) \quad (1)$$

where $E(Co)$, $E(Al)$, $E(W)$, and $E(Co_{1-x-y}Al_xW_y)$ are, respectively, the first-principles calculated total energies (per atom) of ferromagnetic hcp Co, fcc Al, bcc W, and the corresponding alloy, each relaxed to their equilibrium geometries. For binary Co_3Al , none of the structures we consider is energetically more stable than a mechanical mixture of B2 $CoAl$ and hcp Co. Such a conclusion agrees with a recent first-principles study by Mihalkovic and Widom [15], and is also consistent with the fact that no stable compound

with Co_3Al stoichiometry has been observed in the Co-Al system [1]. In accordance with experiments [1], our calculations also confirm hexagonal D0_{19} to be the ground state structure for Co_3W . Our calculated formation energy of Co_3W (-0.08 eV/atom) is in good agreement with the value (-0.05 eV/atom) from a recent thermodynamic assessment of the Co-W binary system by Markstrom *et al.* [16]. For the ternary $\text{Co}_3\text{Al}_{0.5}\text{W}_{0.5}$ alloy, we find that the experimentally observed cubic L1_2 structure is only slightly more stable than the hexagonal D0_{19} structure. Such a small energy difference can be understood since the only difference between the D0_{19} structure and the L1_2 structure is the stacking sequence of hexagonal layers: ABAB... in D0_{19} and ABCABC... in L1_2 . Interestingly, our calculations suggest that $\text{L1}_2\text{-Co}_3\text{Al}_{0.5}\text{W}_{0.5}$ is not thermodynamically stable at low temperatures since its formation energy remains ~ 0.07 eV/atom higher than that of a mixture of B2 CoAl, hcp Co, and D0_{19} Co_3W . We note that, our calculations using the local density approximation (LDA) lead to the same conclusion. For L1_2 and D0_{19} structures, calculations using SQS-1 and SQS-2 structures also give rather similar results (see inset in Fig. 2), which further underlines the validity of the SQS approach. Presumably, the appearance of such a structure at high temperatures is due to entropy (configurational, vibrational, etc.) stabilization effects, similar to the case of Al_2Cu [17]. Furthermore, the effects of short-range ordering, which is completely neglected in our SQS calculations, can play an important role in stabilizing the $\text{L1}_2\text{-Co}_3\text{Al}_{0.5}\text{W}_{0.5}$ phase at finite temperatures. A full account of such effects requires phonon calculations as well as Monte-Carlo simulations using the cluster expansion technique, which is beyond the scope of the present work. We also wish to note that, despite its thermodynamic instability, the

$L1_2\text{-Co}_3\text{Al}_{0.5}\text{W}_{0.5}$ compound can still exist at low temperatures since its decomposition may be kinetically prohibited due to sluggish atomistic diffusion.

To gain more insight into the phase stability of the $L1_2\text{-Co}_3\text{Al}_{0.5}\text{W}_{0.5}$ compound, we have further calculated its total and partial electronic density of states (DOS). As shown in Fig. 3(a), the general feature of the total DOS is the presence of a deep valley near the Fermi level called a “pseudogap” [18, 19], which separates the bonding states from the antibonding states. This pseudogap is mainly due to d - d hybridization between Co and W atoms (see Fig. 3(b)) and indicates the existence of directional covalent bonding in $L1_2\text{-Co}_3\text{Al}_{0.5}\text{W}_{0.5}$. It can be seen that the Fermi level falls below the pseudogap and thus not all the bonding states are filled, which may explain the low structural stability of this compound.

Since our $L1_2$ SQS-2 structure has cubic symmetry, it can be conveniently employed to compute the c_{ij} 's of $L1_2\text{-Co}_3\text{Al}_{0.5}\text{W}_{0.5}$. We extract the elastic constants using an energy-strain approach, *i.e.*, by applying a small strain to the equilibrium lattice and computing the resultant change in total energy [20, 21]. To obtain the bulk modulus B and equilibrium volume, we fit the first-principles calculated total energies at seven different volumes to a third-order Birch-Murnaghan equation of state. The equilibrium lattice constant of $L1_2\text{-Co}_3\text{Al}_{0.5}\text{W}_{0.5}$ is predicted to be 3.582 Å, in good agreement with the experimental value of 3.599 Å [2]. We use a volume-conserving orthorhombic and monoclinic strain to extract the tetragonal shear modulus $\frac{1}{2}(c_{11} - c_{12})$ and the trigonal shear modulus c_{44} , respectively [21]. At each given strain, we fully relax all internal

atomic positions while holding the distorted lattice vectors fixed. Table 2 summarizes our calculated c_{ij} 's of $L1_2\text{-Co}_3\text{Al}_{0.5}\text{W}_{0.5}$. For the purpose of comparison, we have also predicted the c_{ij} 's of the $L1_2\text{-Co}_3\text{Ge}_{1-x}\text{W}_x$ compound [22] at composition $x=0.5$. Both compounds are mechanically stable since their elastic constants obey the elastic stability criteria for a cubic structure: $c_{11} > |c_{12}|$, $c_{44} > 0$, and $c_{11} + 2c_{12} > 0$. Remarkably, our calculated c_{ij} 's of $L1_2\text{-Co}_3\text{Al}_{0.5}\text{W}_{0.5}$ show excellent agreement with the recent experimental measurements by Tanaka *et al.* [23]. From the calculated c_{ij} 's, the polycrystalline shear modulus G and Young's modulus Y are estimated by the Voigt-Reuss-Hill approximation. Both compounds have a B/G ratio larger than 1.75 and are thus likely to be ductile according to the empirical Pugh criterion [24]. This conclusion is further supported by the fact that both structures exhibit a positive Cauchy pressure $c_{12}-c_{44}$ (see Table 2), indicating a predominance of metallic bonding [25]. In comparison, while $L1_2\text{-Co}_3\text{Ge}_{0.5}\text{W}_{0.5}$ has larger bulk and shear moduli and will thus have a stronger strengthening effect than $L1_2\text{-Co}_3\text{Al}_{0.5}\text{W}_{0.5}$, we expect it to be less ductile in view of its lower B/G ratio. Finally, Table 2 reports the shear anisotropic factors $A = 2c_{44}/(c_{11} - c_{12})$ of those two compounds. We find $L1_2\text{-Co}_3\text{Al}_{0.5}\text{W}_{0.5}$ to be elastically more anisotropic than $L1_2\text{-Co}_3\text{Ge}_{0.5}\text{W}_{0.5}$. The ratios Y_{110}/Y_{100} and Y_{111}/Y_{100} are also given in Table 2. Here Y_{hkl} denotes Young's modulus along an arbitrary $[hkl]$ direction. In both compounds, $[100]$ is the softest direction, which helps to explain the experimentally observed fcc+ $L1_2$ two-phase microstructure with cuboidal $L1_2$ precipitates aligned along $\langle 100 \rangle$ directions [2, 3].

In summary, first-principles SQS calculations have been performed to investigate the phase stability and elastic properties of the $L1_2\text{-Co}_3\text{Al}_{0.5}\text{W}_{0.5}$ compound. Unlike Ni_3Al , calculations using both GGA and LDA indicate that $L1_2\text{-Co}_3\text{Al}_{0.5}\text{W}_{0.5}$ is not thermodynamically stable at $T=0\text{K}$ since it is energetically unstable with respect to phase separation into B2 CoAl , hcp Co , and D0_{19} Co_3W . Presumably, its presence at high temperatures is stabilized by entropy as well as short-range ordering effects. Our calculated single-crystal elastic constants of $L1_2\text{-Co}_3\text{Al}_{0.5}\text{W}_{0.5}$ show excellent agreement with experiments. Both calculations and experiments suggest that $L1_2\text{-Co}_3\text{Al}_{0.5}\text{W}_{0.5}$ is ductile. We hope that our calculations can provide guidance for the future development of Co-based superalloys.

ACKNOWLEDGEMENTS

The author acknowledges the support of Director's postdoctoral fellowship at Los Alamos National Laboratory (LANL). All calculations were performed using the parallel computing facilities at LANL.

REFERENCES

- [1] Massalski TB. Binary Alloy Phase Diagrams, 2nd Edition. Metal Park, OH: ASM, 1990.
- [2] Sato J, Omori T, Oikawa K, Ohnuma I, Kainuma R, Ishida K. Science 2006;312:150.
- [3] Suzuki A, Denolf GC, Pollock TM. Scripta Mater 2007;56:385.
- [4] Kresse G, Joubert J. Phys. Rev. B 1999;59:1758.
- [5] Perdew JP, Burke K, Ernzerhof M. Phys. Rev. Lett. 1996;77:3865.
- [6] Kresse G, Furthmuller J. Phys. Rev. B 1996;54:11169.
- [7] Jiang C. Appl. Phys. Lett. 2008;92:041909.
- [8] Zunger A, Wei SH, Ferreira LG, Bernard JE. Phys. Rev. Lett. 1990;65:353.
- [9] Wei SH, Ferreira LG, Bernard JE, Zunger A. Phys. Rev. B 1990;42:9622.
- [10] Gyorffy BL. Phys. Rev. B 1972;5:2382.
- [11] Mikkelsen JC, Boyce JB. Phys. Rev. Lett. 1982;49:1412.
- [12] Jiang C, Wolverton C, Sofo J, Chen LQ, Liu ZK. Phys. Rev. B 2004;69:214202.
- [13] Jiang C, Chen LQ, Liu ZK. Acta Mater 2005;53:2643.
- [14] van de Walle A, Asta M, Ceder G. Calphad 2003;26:539.
- [15] Mihalkovic M, Widom M. Phys. Rev. B 2007;75:014207.
- [16] Markstrom A, Sundman B, Frisk K. J. Phase Equil. 2005;26:152.
- [17] Wolverton C, Ozolins V. Phys. Rev. Lett. 2001;86:5518.
- [18] Lin W, Xu JH, Freeman AJ. Phys. Rev. B 1992;45:10863.
- [19] Xu JH, Lin W, Freeman AJ. Phys. Rev. B 1993;48:4276.

- [20] Jiang C, Srinivasan SG, Caro A, Maloy SA. *J. Appl. Phys.* 2008;103:043502.
- [21] Jiang C, Sordelet DJ, Gleeson B. *Acta Mater* 2006;54:2361.
- [22] Chinen H, Sato J, Omori T, Oikawa K, Ohnuma I, Kainuma R, Ishida K. *Scripta Mater* 2007;56:141143.
- [23] Tanaka K, Ohashi T, Kishida K, Inui H. *Appl. Phys. Lett.* 2007;91:181907.
- [24] Pugh SF. *Philos. Mag.* 1954;45:823.
- [25] Pettifor DG. *Mater. Sci. Technol.* 1992;8:345.

Table 1. Pair and three-body correlation functions of 32-atom SQS's for mimicking random $A_3B_{0.5}C_{0.5}$ alloys with $L1_2$, $D0_{19}$, and $D0_3$ crystal structures, respectively.

Structure	$\bar{\Pi}_{2,1}$	$\bar{\Pi}_{2,2}$	$\bar{\Pi}_{2,3}$	$\bar{\Pi}_{2,4}$	$\bar{\Pi}_{2,5}$	$\bar{\Pi}_{2,6}$	$\bar{\Pi}_{3,1}$	$\bar{\Pi}_{3,2}$
Random Alloy	0	0	0	0	0	0	0	0
$L1_2$ SQS-1	0	0	0	-0.3333	0	0	-	0
$L1_2$ SQS-2	0	0	-1	1	0	0	-	0
$D0_{19}$ SQS-1	0	0	0	0	-0.3333	0	-	0
$D0_{19}$ SQS-2	0	0	-0.3333	0	0	0	-	0
$D0_3$ SQS	0	0	-0.1667	0.3333	0	0	0	0

Table 2. Single-crystal elastic constants (in GPa) of L1₂-Co₃Al_{0.5}W_{0.5} and L1₂-Co₃Ge_{0.5}W_{0.5} compounds from first-principles calculations and experiments. Isotropic polycrystalline elastic moduli, the Cauchy pressure, and the elastic anisotropy parameters are also shown.

Structure	c_{11}	c_{12}	c_{44}	B	G	Y	B/G	$c_{12} - c_{44}$	A	Y_{110}/Y_{100}	Y_{111}/Y_{100}
Co ₃ Al _{0.5} W _{0.5} ^a	264	162	153	196	99	253	1.99	9	2.89	1.85	2.59
Co ₃ Al _{0.5} W _{0.5} ^b	271	172	162	205	101	260	2.03	10	3.26	1.94	2.80
Co ₃ Ge _{0.5} W _{0.5} ^a	371	186	177	248	136	346	1.82	9	1.91	1.47	1.74

^aFrom the present first-principles SQS calculations.

^bExperimental results from Tanaka *et al.*[23]

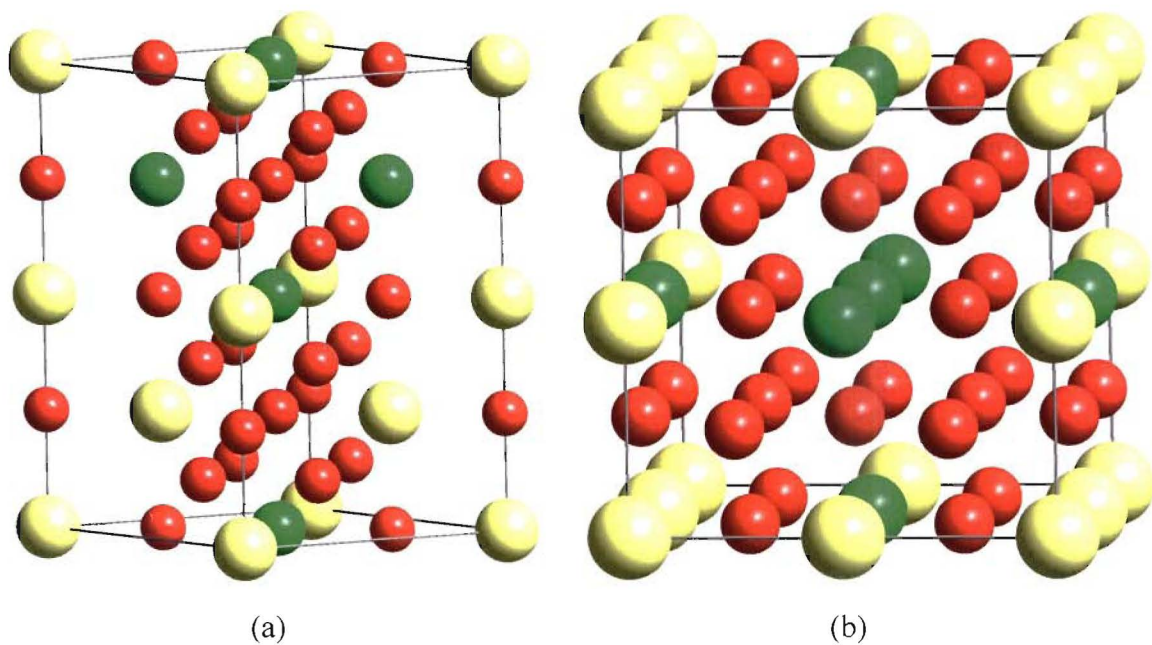


FIG. 1. 32-atom SQS-1 (a) and SQS-2 (b) structures for representing $A_3B_{0.5}C_{0.5}$ alloys with $L1_2$ crystal structure. Red, yellow and white spheres represent A, B and C atoms, respectively.

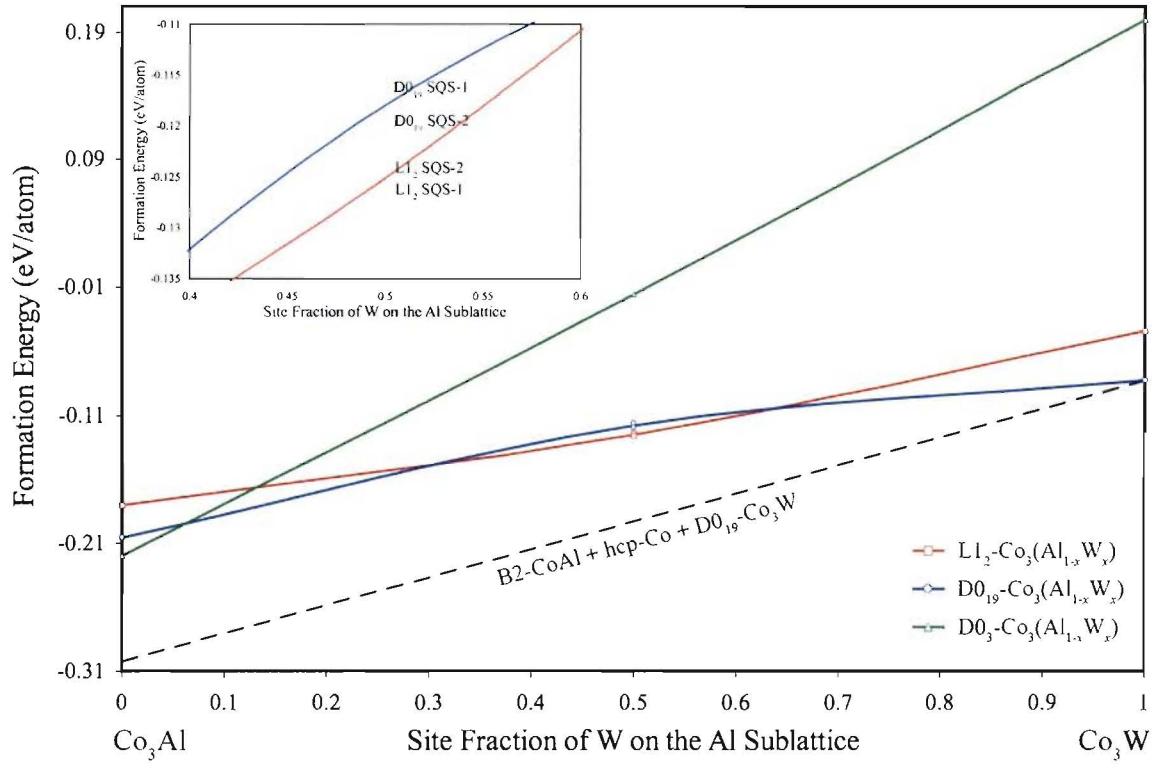


FIG. 2. First-principles calculated formation energies of $\text{Co}_3\text{Al}_{1-x}\text{W}_x$ alloys in various competing crystal structures. The dashed line denotes the formation energy of a mechanical mixture of B2 CoAl, hcp Co, and $\text{D0}_{19}\text{Co}_3\text{W}$ with the same composition. Fcc Al, bcc W, and ferromagnetic hcp Co are used as reference states for the pure elements.

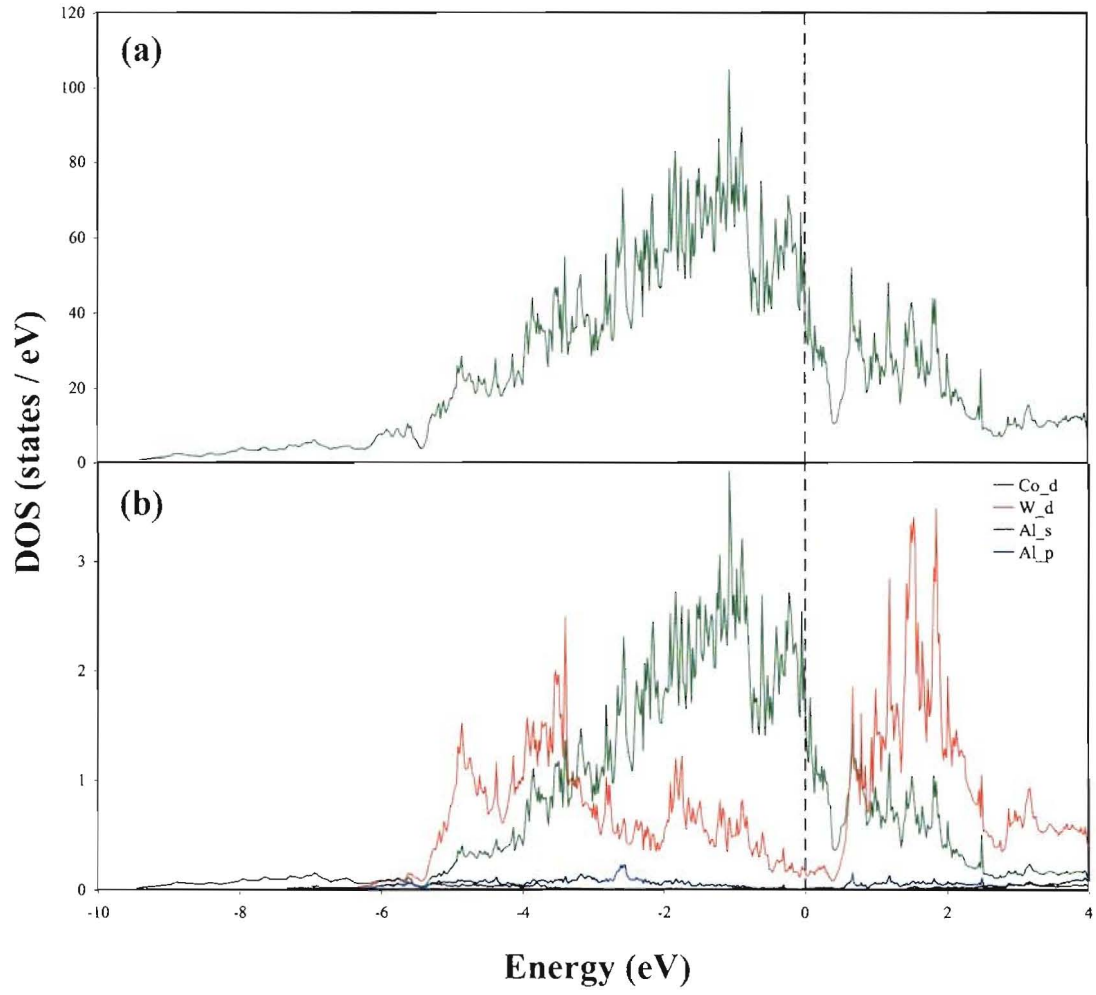


FIG. 3. Total (a) and site and angular momentum projected (b) electronic density of states of $L1_2\text{-Co}_3\text{Al}_{0.5}\text{W}_{0.5}$. The vertical line denotes the Fermi level.